


Distributed Lagrange Multiplier Functions for Fictitious Domain Method with Spectral/hp Element Discretization

Riccardo Zamolo¹  · Lucia Parussini¹ ·
Valentino Pediroda¹

Accepted: 18 May 2017

Abstract A fictitious domain approach for the solution of second-order linear differential problems is proposed; spectral/hp elements have been used for the discretization of the domain. The peculiarity of our approach is that the Lagrange multipliers are particular distributed functions, instead of classical δ Dirac (impulsive) multipliers. In this paper we present the formulation and the application of this approach to 1D and 2D Poisson problems and 2D Stokes flow (biharmonic equation).

Keywords Fictitious domain · Lagrange multipliers · Spectral/hp element method · Poisson problem · Biharmonic problem

Mathematics Subject Classification 65L10 · 65N35

1 Introduction

A fictitious domain approach to solve a differential problem consists in an extension of the domain of the problem to a larger and simple shaped one. This choice brings some advantages: a specific geometry dependent mesh is no longer needed because a simple uniform structured mesh can be used, allowing the employment of efficient solvers. Several works with application to engineering relevant problems have been proposed [1–4], highlighting the potentialities of the fictitious domain approach when coupled with finite element/finite difference methods.

✉ Riccardo Zamolo
riccardo.zamolo@phd.units.it

Lucia Parussini
lparussini@units.it

Valentino Pediroda
pediroda@units.it

¹ Engineering and Architecture Department, University of Trieste, Via A. Valerio 10, 34127 Trieste, Italy

Alongside the previous approach, the development of the spectral/*hp* element method (SEM) [5–8], a discretization technique which uses high order expansions for the solution of differential problems, have suggested the coupling of the SEM with a fictitious domain approach. Different types of specific schemes have been proposed [9]; in this paper we focus our attention on the use of Lagrange multipliers [10–13] where steady state problems are successfully solved.

Classical approaches use impulsive Dirac multipliers displaced over the original boundary to satisfy the boundary conditions (BCs); this choice leads to some problems when dealing with high order methods, which require a certain degree of regularity of domains and data [7], and some stability problems in time dependent simulations. In this paper we will investigate the case of distributed Lagrange multiplier functions which we expect to remove or reduce the troubles observed in the concentrated Lagrange multipliers approach when coupled to high order methods.

The use of distributed Lagrange multipliers with a fictitious domain approach has already been investigated [14–16]; an exhaustive study of this approach can be found in [17] within a finite element framework. Dong et al. [18] employed a distributed Lagrange multiplier approach within a spectral/*hp* element framework to simulate flows past obstacles by forcing Gaussian multipoles distributed over the obstacles volume, while [19] investigated the use of distributed Lagrange multipliers functions with a specific spectral method where a single global expansion was used.

In this paper the coupling of the spectral/*hp* element method with a fictitious domain approach, in the case of distributed Lagrange multiplier functions, will be investigated in terms of convergence rates of computed solutions for a certain number of 1D and 2D test cases, for which reasonable convergence rates are possible when using particular distributed functions.

2 Second-Order Differential Problem

Let ω be a closed bounded region of \mathbb{R} (1D case) or \mathbb{R}^2 (2D case), and $\gamma = \partial\omega$ its boundary. In a general form, a second-order differential problem can be expressed as follows: find $u(\mathbf{x})$, $\mathbf{x} \in \omega$, such that

$$\mathcal{D}(u) = b \quad \text{in } \omega \tag{1}$$

$$u = \bar{u} \quad \text{on } \gamma_D \tag{2}$$

$$\mathbf{A}\nabla u \cdot \mathbf{n} = \bar{q} \quad \text{on } \gamma_N \tag{3}$$

where \mathcal{D} is a second-order linear differential operator, b is the source term, γ_D is the portion of γ where u assumes the prescribed value \bar{u} (Dirichlet BC), γ_N is the portion of γ where the outward flux $\mathbf{A}\nabla u \cdot \mathbf{n}$ assumes the prescribed value \bar{q} (Neumann BC), \mathbf{A} is the flux tensor and \mathbf{n} is the outward unit normal on γ .

3 Spectral/*hp* Element Method

The spectral/*hp* element method (see [7]) for the approximation of the previous problem (1)–(3) uses a high order finite expansion of the solution, defined locally on each portion of the domain (elements). In this paper the elements, denoted by e , are uniform segments in 1D

and uniform squares in 2D, thanks to the fictitious domain approach which allows the use of simple uniform structured meshes.

The main advantage of this method over traditional finite volume/finite element methods is the exponential convergence as the expansion order increases.

In 1D cases, assumed $\xi \in [-1, 1]$ the non-dimensional coordinate over the element, the chosen local modal basis is

$$\phi_i(\xi) = \begin{cases} (1 - \xi)/2 & i = 0 \\ (1 + \xi)/2 & i = 1 \\ J_{i-2}^{1,1}(\xi)(1 - \xi)(1 + \xi)/4 & 2 \leq i \leq P \end{cases} \quad (4)$$

which is a polynomial basis of order P , where $J_{i-2}^{1,1}$ is the Jacobi polynomial of order $i - 2$ and parameters are $\alpha = 1, \beta = 1$ (see [7]).

The solution is then approximated by the following local expansion on each element e

$$u_e^*(\xi) = \sum_{i=0}^P \hat{u}_i^{(e)} \phi_i(\xi) \quad (5)$$

where $\hat{u}_i^{(e)}$ are the unknown coefficients of the local 1D expansion.

For 2D cases the local basis is the tensor product of 1D basis functions; assumed $(\xi, \eta) \in [-1, 1] \times [-1, 1]$ the non-dimensional coordinates over the element e , the local expansion is therefore

$$u_e^*(\xi, \eta) = \sum_{i,j=0}^P \hat{u}_{ij}^{(e)} \phi_i(\xi) \phi_j(\eta) \quad (6)$$

where $\hat{u}_{ij}^{(e)}$ are the unknown coefficients of the local 2D expansion.

The final set of discrete equations is then obtained by the application of the Galerkin method, which orthogonalizes the global error of (1) for the approximation u^* locally defined by (5) or (6) with respect to each free global basis function Φ_k (which is the global composition of local free modes over each element) on the domain ω

$$\int_{\omega} [\mathcal{D}(u^*) - b] \Phi_k \, d\omega = 0 \quad (7)$$

for $k = 1, \dots, N$ where N is the total number of unknown coefficients.

Using compact matrix notation, (7) writes

$$\mathbf{D}\hat{\mathbf{u}} = \hat{\mathbf{b}} \quad (8)$$

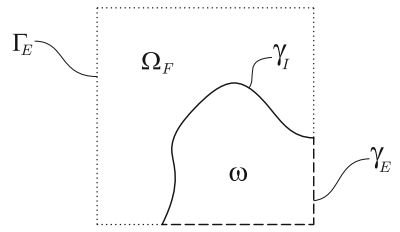
where \mathbf{D} is the $N \times N$ coefficient matrix, $\hat{\mathbf{u}}$ is the $N \times 1$ unknown global vector of expansion coefficients and $\hat{\mathbf{b}}$ is the $N \times 1$ source term vector; the BCs are included in this formulation (see [7] for details).

The relation between local and global vectors of expansion coefficients is given by

$$\hat{\mathbf{u}}^{(e)} = \mathbf{C}_e \hat{\mathbf{u}} \quad (9)$$

where \mathbf{C}_e is the connectivity matrix of element e .

Fig. 1 Original domain ω , fictitious domain Ω_F , external fictitious boundary Γ_E , immersed boundary γ_I and external boundary γ_E



4 Fictitious Domain Approach

4.1 Analytical Formulation

The fictitious domain approach extends the original differential problem, defined on an irregular shaped domain ω , to a larger and simply shaped extended domain Ω ; the fictitious domain is therefore $\Omega_F = \Omega \setminus \omega$, that is the portion of Ω outside ω (see Fig. 1).

The extended domain boundary is $\Gamma = \partial\Omega$, the external boundary of the original domain is $\gamma_E = \gamma \cap \Gamma$, the external boundary of the fictitious domain is $\Gamma_E = \Gamma \setminus \gamma_E$ and the immersed boundary of the original domain is $\gamma_I = \gamma \setminus \gamma_E$.

The original boundary conditions prescribed on γ_I have to be enforced as constraints in the new extended problem, since this portion of the original boundary is now immersed in the extended domain.

Since the fictitious domain has its own external boundary Γ_E , new boundary conditions have to be prescribed therein; therefore these fictitious BCs can virtually assume arbitrary values.

Under this assumptions the original problem (1)–(3) can be expressed as follows: find $u(\mathbf{x})$ and $b_F(\mathbf{x})$, $\mathbf{x} \in \Omega$, such that

$$\mathcal{D}(u) = b + b_F \quad \text{in } \Omega \quad (10)$$

$$u = \tilde{u} \quad \text{on } \Gamma_{E,D} \quad (11)$$

$$\mathbf{A}\nabla u \cdot \mathbf{n} = \tilde{q} \quad \text{on } \Gamma_{E,N} \quad (12)$$

$$u = \bar{u} \quad \text{on } \gamma_D \quad (13)$$

$$\mathbf{A}\nabla u \cdot \mathbf{n} = \bar{q} \quad \text{on } \gamma_N \quad (14)$$

where b_F is the unknown fictitious source term satisfying $b_F = 0$ in ω to guarantee the equivalence between the original problem and the new problem; $\Gamma_{E,D}$ is the portion of Γ_E where the arbitrary value \tilde{u} is imposed and $\Gamma_{E,N}$ is the portion of Γ_E where the arbitrary flux \tilde{q} is imposed.

It is important to notice that conditions (13)–(14) referring to $\gamma_I \subseteq (\gamma_D \cup \gamma_N)$ are to be intended as constraints for the new problem: the role of the unknown fictitious source term b_F is therefore to satisfy the constrained part of these boundary conditions referring to the immersed boundary γ_I .

We define $\gamma_{I,D}$ as the portion of γ_I where Dirichlet BCs are imposed and $\gamma_{I,N}$ as the portion of γ_I where Neumann BCs are imposed.

4.2 Discrete Formulation

At a discrete level the fictitious term b_F is chosen to be a linear combination of a finite number M of generic functions g_i distributed over the fictitious domain

$$b_F = \sum_{j=1}^M \lambda_j g_j \quad (15)$$

where λ_j are the M unknown multipliers and $g_j = 0$ on ω for each $j = 1, \dots, M$. The application of the Galerkin spectral discretization (7) on global error of (10) yields the following linear system

$$\mathbf{D}\hat{\mathbf{u}} = \hat{\mathbf{b}} + \hat{\mathbf{Q}}\boldsymbol{\lambda} \quad (16)$$

where the components of $N \times M$ matrix $\hat{\mathbf{Q}}$ are given by

$$\hat{Q}_{kj} = \int_{\omega} \Phi_k g_j d\omega \quad (17)$$

while $\boldsymbol{\lambda}$ is the $M \times 1$ unknown multipliers vector $\{\lambda_1, \dots, \lambda_M\}^T$ and the j th column of $\hat{\mathbf{Q}}$ will be denoted by $\hat{\mathbf{q}}_j$; let us notice the distributed functions g_i can assume the most generic form.

The global system is then closed writing the discretized version of constrained part of original BCs expressed by (13)–(14) as follows.

4.2.1 1D Cases

The immersed boundary γ_I is composed by M single points \bar{x}_i , each one requiring one single BC and thus requiring one single multiplier. Therefore the constrained part of (13) and (14) can be written explicitly as follows

$$\mathbf{B}\hat{\mathbf{u}} = \bar{\mathbf{u}} \quad (18)$$

where $\bar{\mathbf{u}}$ is the $(P + 1) \times 1$ vector of the prescribed boundary values, *i.e.*, the right hand side of (13) or (14) depending upon the type of BC prescribed in each \bar{x}_i , while \mathbf{B} is the $M \times N$ matrix whose rows \mathbf{B}_i are

$$\mathbf{B}_i = \boldsymbol{\phi}_i \mathbf{C}_{e(i)} \quad (19)$$

and $e(i)$ is the element on which \bar{x}_i lies.

The components of the $1 \times (P + 1)$ vector $\boldsymbol{\phi}_i$ are given by the values of the local basis functions or their spatial derivatives times the outward unit normal (± 1 in 1D) in $x = \bar{x}_i$, depending upon the type of BC prescribed in \bar{x}_i .

The final system is then formed combining (16) and (18)

$$\begin{bmatrix} \mathbf{D} & -\hat{\mathbf{Q}} \\ \mathbf{B} & \mathbf{0} \end{bmatrix} \begin{bmatrix} \hat{\mathbf{u}} \\ \boldsymbol{\lambda} \end{bmatrix} = \begin{bmatrix} \hat{\mathbf{b}} \\ \bar{\mathbf{u}} \end{bmatrix} \quad (20)$$

An efficient way to solve the final system (20) requires the Schur complement of \mathbf{D} , *i.e.*, the orthogonalization of the global system in order to obtain a reduced system whose only unknown is the multipliers vector $\boldsymbol{\lambda}$

$$\mathbf{B}\mathbf{D}^{-1}\hat{\mathbf{Q}}\boldsymbol{\lambda} = \bar{\mathbf{u}} - \mathbf{B}\mathbf{D}^{-1}\hat{\mathbf{b}} \quad (21)$$

Once (21) has been solved in $\boldsymbol{\lambda}$, the final solution $\hat{\mathbf{u}}$ can be computed solving (16).

4.2.2 2D Cases

The immersed boundary γ_I is a curve and it is not possible to satisfy exactly the constrained BCs on it, because of the finite number M of available multipliers. The possible solutions are two: to choose M points on γ_I and write one BC constraint for each point in a collocation fashion, or to impose a minimum condition between the prescribed BC and the effective values/fluxes of the solution along γ_I .

We chose the latter solution because collocation on fixed points can exhibit problems when dealing with high order polynomials (Runge's phenomenon); the minimum condition writes

$$\min_{\lambda \in \mathbb{R}^M} \left[\int_{\gamma_{I,D}} (u^* - \bar{u})^2 d\gamma + \int_{\gamma_{I,N}} (\mathbf{A}\nabla u^* \cdot \mathbf{n} - \bar{q})^2 d\gamma \right] \quad (22)$$

Let e_1, \dots, e_R be the elements which intersect the immersed boundary γ_I , and consequently $\gamma_{D,i} = \gamma_{I,D} \cap e_i$ and $\gamma_{N,i} = \gamma_{I,N} \cap e_i$ are, respectively, the portions of $\gamma_{I,D}$ and $\gamma_{I,N}$ lying on e_i for $i = 1, \dots, R$; obviously we have $\gamma_{I,D} = \cup \gamma_{D,i}$ and $\gamma_{I,N} = \cup \gamma_{N,i}$.

Since the solution is expressed by an analytical expansion as in (6), it is possible to impose null partial derivatives of the previous BC error given by (22) respect to each multiplier λ_k

$$\begin{aligned} f_k(\boldsymbol{\lambda}) &:= \frac{\partial}{\partial \lambda_k} \left[\int_{\gamma_{I,D}} (u^* - \bar{u})^2 d\gamma + \int_{\gamma_{I,N}} (\mathbf{A}\nabla u^* \cdot \mathbf{n} - \bar{q})^2 d\gamma \right] \\ &= 2 \sum_{i=1}^R \left[\int_{\gamma_{D,i}} (u_{e_i}^* - \bar{u}) \frac{\partial u_{e_i}^*}{\partial \lambda_k} d\gamma + \int_{\gamma_{N,i}} (\mathbf{A}\nabla u_{e_i}^* \cdot \mathbf{n} - \bar{q}) \frac{\partial}{\partial \lambda_k} (\mathbf{A}\nabla u_{e_i}^* \cdot \mathbf{n}) d\gamma \right] = 0 \end{aligned} \quad (23)$$

for $k = 1, \dots, M$. From (9) and (16) we have

$$\hat{\mathbf{u}}^{(e_i)} = \mathbf{C}_e \mathbf{D}^{-1} [\hat{\mathbf{b}} + \hat{\mathbf{Q}}\boldsymbol{\lambda}] = \mathbf{C}_e [\hat{\mathbf{u}}_0 + \hat{\mathbf{U}}\boldsymbol{\lambda}] \quad (24)$$

where $\hat{\mathbf{u}}_0 = \mathbf{D}^{-1}\hat{\mathbf{b}}$ and $\hat{\mathbf{U}} = \mathbf{D}^{-1}\hat{\mathbf{Q}}$; (24) states that the expansion coefficients $\hat{\mathbf{u}}^{(e_i)}$ of $u_{e_i}^*$ in (23) has linear dependence on $\boldsymbol{\lambda}$ and therefore (23) can be written in the following compact form

$$\mathbf{f}(\boldsymbol{\lambda}) = \mathbf{L}\boldsymbol{\lambda} + \mathbf{f}_0 = \mathbf{0} \quad (25)$$

where $\mathbf{f}(\boldsymbol{\lambda}) = \{f_1(\boldsymbol{\lambda}), \dots, f_M(\boldsymbol{\lambda})\}^T$ is the $M \times 1$ vector of derivatives defined by (23), \mathbf{L} is a $M \times M$ coefficient matrix (whose columns will be denoted by \mathbf{L}_j) and $\mathbf{f}_0 = \mathbf{f}(\mathbf{0})$.

$\hat{\mathbf{u}}_0$, \mathbf{L} and \mathbf{f}_0 can be computed through Algorithm 1 using the partial derivatives of (24) as follows

$$\frac{\partial \hat{\mathbf{u}}^{(e_i)}}{\partial \lambda_k} = \mathbf{C}_e \hat{\mathbf{u}}_k \quad (26)$$

where $\hat{\mathbf{u}}_k$ is the k th column of $\hat{\mathbf{U}}$ for $k = 1, \dots, M$.

The evaluation of path integrals in (23), requested by Algorithm 1 at lines 6 and 14, is accomplished through a standard numerical quadrature algorithm; it is worth noting that the linear systems to be solved at lines 1 and 3 have the same coefficient matrix \mathbf{D} .

Once \mathbf{L} and \mathbf{f}_0 have been computed, (25) can be solved in $\boldsymbol{\lambda}$ and, finally, the global vector of expansion coefficients can be directly computed from the global equivalent of (24).

$$\hat{\mathbf{u}} = \hat{\mathbf{u}}_0 + \hat{\mathbf{U}}\boldsymbol{\lambda}. \quad (27)$$

Algorithm 1 Evaluation of $\hat{\mathbf{u}}_0$, \mathbf{L} and \mathbf{f}_0

```
1: Solve  $\hat{\mathbf{u}}_0$  from  $\mathbf{D}\hat{\mathbf{u}}_0 = \hat{\mathbf{b}}$ 
2: for  $k = 1, \dots, M$  do
3:   Solve  $\hat{\mathbf{u}}_k$  from  $\mathbf{D}\hat{\mathbf{u}}_k = \hat{\mathbf{q}}_k$ 
4: end for ▷  $\hat{\mathbf{U}}$  has been evaluated
5: for  $k = 1, \dots, M$  do
6:   Evaluate  $f_k(\mathbf{0})$  from (23) using  $\mathbf{C}_{e_i}\hat{\mathbf{u}}_0$  for  $u_{e_i}^*$  and (26) for  $\partial u_{e_i}^*/\partial \lambda_k$ 
7: end for ▷  $\mathbf{f}(\mathbf{0})$  has been evaluated
8:  $\mathbf{f}_0 \leftarrow \mathbf{f}(\mathbf{0})$ 
9: for  $j = 1, \dots, M$  do
10:   $\boldsymbol{\lambda} \leftarrow \mathbf{0}$ 
11:   $\lambda_j \leftarrow 1$ 
12:   $\hat{\mathbf{u}} \leftarrow \hat{\mathbf{u}}_0 + \hat{\mathbf{u}}_j$ 
13:  for  $k = 1, \dots, M$  do
14:    Evaluate  $f_k(\boldsymbol{\lambda})$  from (23) using  $\mathbf{C}_{e_i}\hat{\mathbf{u}}$  for  $u_{e_i}^*$  and (26) for  $\partial u_{e_i}^*/\partial \lambda_k$ 
15:  end for ▷  $\mathbf{f}(\boldsymbol{\lambda})$  has been evaluated
16:   $\mathbf{L}_j \leftarrow \mathbf{f}(\boldsymbol{\lambda}) - \mathbf{f}_0$ 
17: end for ▷  $\mathbf{L}$  has been evaluated
```

4.3 Computational Costs

The proposed procedure requires the solution of $M + 1$ linear systems (Algorithm 1 at lines 1 and 3), and the numerical quadrature of M^2 path integrals (Algorithm 1 at lines 6 and 14) where M is the number of multipliers.

This additional costs may seem high, compared to the standard approach with geometry dependent mesh, but it is important to notice the coefficient matrix \mathbf{D} is independent by the geometry of immersed boundary and by the value of the immersed BC, so it can be factored once. Moreover \mathbf{D} has particular properties because of the uniform structured mesh that have been used, allowing the use of efficient solvers.

The cost of the numerical quadratures is also negligible as long as the number of multipliers M is not too high (e.g., ≈ 250 in 2D); this value is also the limit beyond which the matrix \mathbf{L} becomes too ill-conditioned and therefore the constrained BCs (13)–(14) are not accurately satisfied.

5 Results

Some simple test cases have been carried out to validate the proposed approach, comparing the accuracy of computed solutions with analytical solutions available for these cases. First we consider one-dimensional and two-dimensional Poisson equations, then we consider a two-dimensional biharmonic equation (Stokes flow) which has practical applications.

5.1 One-Dimensional Poisson Equation

The topology of the domains ω , Ω_F and Ω is reported in Fig. 2, where 4 spectral elements with same length $h = 0.25$ are used. The original domain is $\omega = (a, 1)$, the fictitious domain is $\Omega_F = (0, a)$ and the immersed boundary is thus the single point $x = a = 1.5h$.

The reference analytical solution u is a harmonic (sinusoidal) function whose spatial period is the length of the original domain $1 - a$

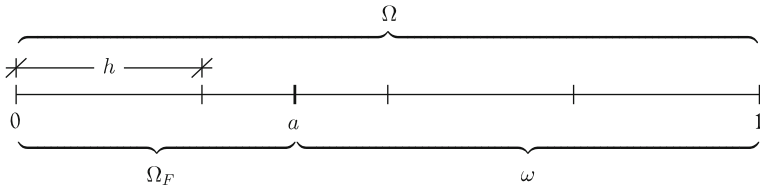


Fig. 2 Domains and discretization for the one-dimensional test case

$$u(x) = \sin\left(2\pi \frac{x-a}{1-a}\right) \quad (28)$$

Let us consider a one-dimensional Poisson problem with zero-valued Dirichlet BCs, i.e., $\mathcal{D}(u) = d^2u/dx^2$ and $\bar{u} = 0$, problem (1)–(2); under the previous assumptions the extended problem (10)–(13) is therefore

$$\frac{d^2u}{dx^2} = -\left(\frac{2\pi}{1-a}\right)^2 \sin\left(2\pi \frac{x-a}{1-a}\right) + \lambda g \quad \text{in } \Omega = (0, 1) \quad (29)$$

$$u = 0 \quad \text{in } x = 0 \quad (30)$$

$$u = 0 \quad \text{in } x = \{a, 1\} \quad (31)$$

where (30) represents the arbitrary BC on the external boundary $\Gamma_E = \{0\}$ of fictitious domain, chosen to be a simple zero-valued Dirichlet BC; (31) represents the BCs of the original problem: this BC referred to $x = a$ is the constrained BC. A fundamental assumption is that the harmonic source term is considered valid over the entire extended domain Ω .

Assumed $\varepsilon = u^* - u$ as the error between the computed solution and the analytical solution, the relative energy norm (see [7]) is defined as

$$\|\varepsilon\|_E = \sqrt{\int_{\omega} \left(\frac{d\varepsilon}{dx}\right)^2 dx} \quad (32)$$

We chose a distributed function $g = (a-x)^i$ for $i \geq 0$ and $x < a$, for which the convergence curves are shown in Fig. 3. The influence of the exponent i is clear: as i increases, the discontinuity in $x = a$ of the derivatives till order $i - 1$ of the global source term, i.e., right hand side of (29), vanishes, and therefore a higher convergence rate can be achieved. As a limit case, we can assume a distributed function g which vanishes on the entire element containing the immersed boundary $x = a$ and having arbitrary distribution on the first element $[0, h]$: in this ideal case a perfectly exponential convergence is achievable.

When the original source term b of (1) is defined only on the original domain ω , it is possible to use a truncated Taylor expansion of b around the immersed boundary $x = a$ to avoid discontinuous derivatives therein

$$b(x) = \sum_{k=0}^n \frac{1}{k!} \left. \frac{d^k b}{dx^k} \right|_{x=a} (x-a)^k \quad x < a \quad (33)$$

Figure 4 shows the convergence curves in the case of Taylor expansion of b for the same problem (29)–(31) for various expansion orders n and $g = 1$ for $x < h$, i.e., the fictitious function g is non-zero only on the first element which doesn't contain the immersed boundary.

Fig. 3 Case $g = (a - x)^i$: convergence curves versus polynomial order P

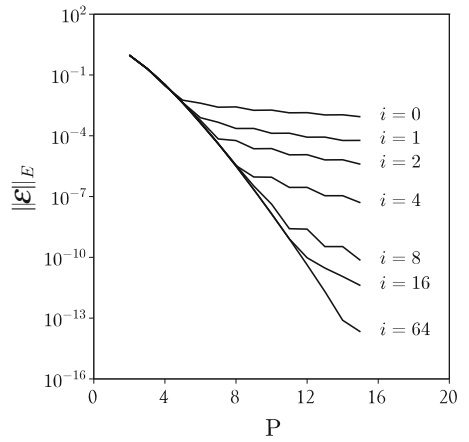
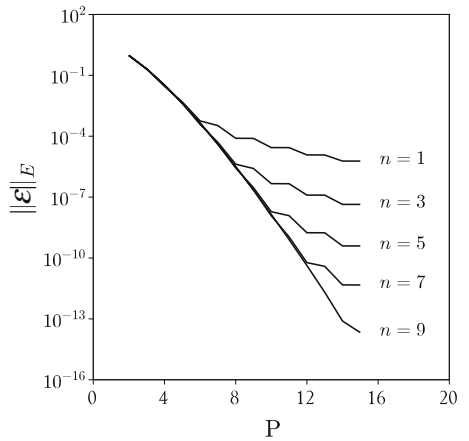


Fig. 4 Series extension of order n of source term b : convergence curves versus polynomial order P



Again, as the order n increases, so the convergence rate does because the global source term has continuous derivatives in $x = a$ till order n . As predictable, these one-dimensional test cases confirm that our approach can provide increasing convergence rates with increasing regularity of the global source term.

5.2 Two-Dimensional Poisson Equation

The topology of the domains is reported in Fig. 5 where 16 uniform spectral elements of side length h are used, 4 for each direction. The original domain ω is the circle of radius R centered in $(0.5, 0.5)$, the extended domain $\Omega = (0, 1) \times (0, 1)$ is the unit square and the fictitious domain $\Omega_F = \Omega \setminus \bar{\omega}$ is therefore the portion of the unit square outside the circle.

The immersed boundary $\gamma_I = \gamma$ is then the circumference of radius R and the adopted radius/elements side length ratio is $R/h = 0.9$ (Fig. 6).

The reference analytical solution is chosen to be a paraboloid centered in the origin of the circle and vanishing on it

$$u(x, y) = R^2 - [(x - 0.5)^2 + (y - 0.5)^2] \quad (34)$$

Fig. 5 Discretization for the two-dimensional test case, b_F is defined only on *dashed* elements

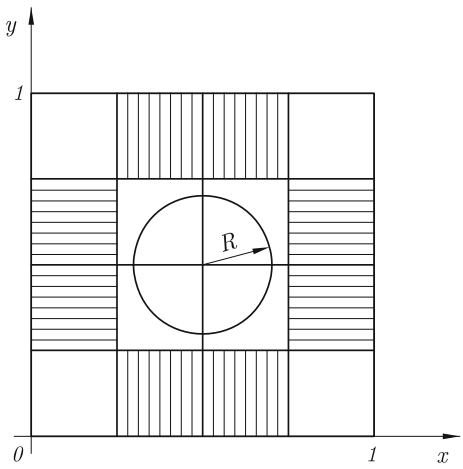
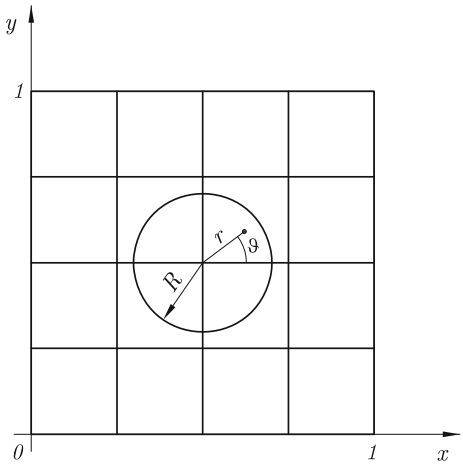


Fig. 6 Discretization for the two-dimensional test case, b_F is defined on the whole Ω_F



Let us consider a two-dimensional Poisson problem with zero-valued Dirichlet BCs, *i.e.*, $\mathcal{D}(u) = \nabla^2 u$ and $\bar{u} = 0$, problem (1)-(2); under the previous assumptions the extended problem (10)-(13) is therefore

$$\nabla^2 u = -4 + b_F \quad \text{in } \Omega = (0, 1) \times (0, 1) \quad (35)$$

$$u = 0 \quad \text{on } \Gamma = \partial\Omega \quad (36)$$

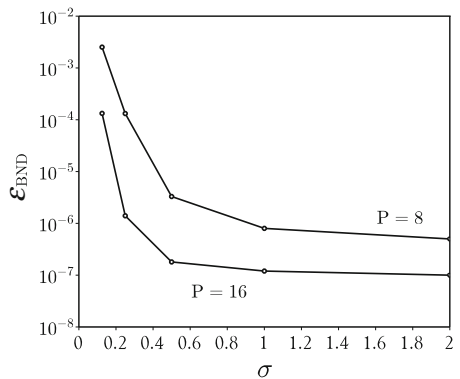
$$u = 0 \quad \text{on } \gamma = \partial\omega \quad (37)$$

where (36) represents the arbitrary (zero-valued Dirichlet) BC on the external fictitious boundary $\Gamma_E = \Gamma$ and (37) represents the BCs of the original problem; again, the constant source term is considered valid over the entire extended domain Ω .

Assumed ε as the previously defined error between computed and analytical solution, the relative energy norm (see [7]) is defined as

$$\|\varepsilon\|_E = \sqrt{\int_{\omega} \|\nabla \varepsilon\|_2^2 d\omega} \quad (38)$$

Fig. 7 Immersed boundary error with $M = 8P\sigma$ multipliers



In this two-dimensional case where a constrained Dirichlet BC is prescribed on γ_I , the boundary error ε_{BND} between the computed solution u^* and the prescribed value $\bar{u} = 0$ along γ_I is defined as

$$\varepsilon_{\text{BND}} = \sqrt{\int_{\gamma_I} u^{*2} d\gamma}. \quad (39)$$

5.2.1 Fictitious Source Term b_F Defined on External Elements

The fictitious functions g_i which define the fictitious source term b_F in (15) are chosen to be vanishing on the elements containing the immersed boundary γ_I , as proposed in the one-dimensional test case.

In particular we choose to use M_e fictitious functions on each of the 8 dashed elements shown in Fig. 5, where each fictitious function assumes a unit constant value on one of each parallel strip. Assumed $\sigma = M_e/P$, with P order of the spectral expansion, the total number of g_i fictitious functions is $M = 8M_e = 8P\sigma$, and thus the total number of multipliers λ_j is also M .

Figure 7 shows the influence of the σ parameter on the ε_{BND} boundary error along γ_I for two expansion orders $P = 8$ and $P = 16$. It is evident that σ values greater than 0.5 have a little influence on ε_{BND} , which possesses an asymptotical behaviour. This is an important characteristic of this case: for a fixed value of P (polynomial expansion order) it's impossible to satisfy the original BC (37) on the immersed boundary with arbitrary accuracy even using a very high number M of multipliers.

A reasonable choice in this case is therefore $\sigma = 0.5$, for which convergence curves are shown in Fig. 8: the exponential convergence is lost, but a reasonable convergence rate is achieved. This loss of exponential convergence is due to the unsatisfied BC along the immersed boundary.

Graphical representations of the global solution for $P = 22$ are given in Fig. 9 where the particular behaviour of the solution on the fictitious domain can be observed.

5.2.2 Fictitious Source Term b_F Defined on Ω_F

We now propose another possible choice for g_i fictitious functions which allows a better resolution of the BC along the immersed boundary; using the polar coordinates (r, ϑ) shown

Fig. 8 Case $\sigma = 0.5$:
convergence curves versus
polynomial order P

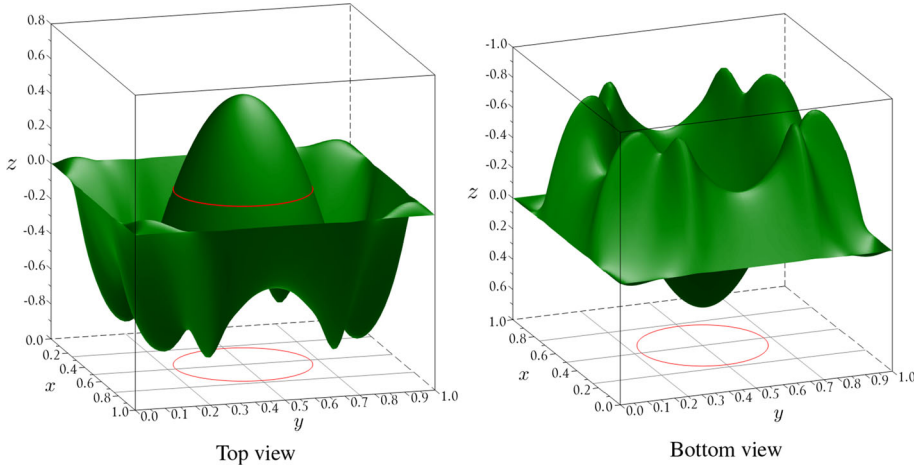
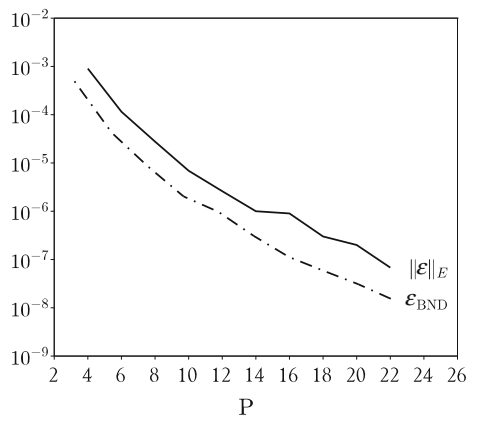


Fig. 9 Global solution with $P = 22$

in Fig. 6, g_i functions are defined as

$$g_i(r, \vartheta) = \begin{cases} (r - R)^d \sin(i\vartheta) & i = 1, \dots, M_\vartheta \\ (r - R)^d \cos[(i - M_\vartheta - 1)\vartheta] & i = M_\vartheta + 1, \dots, 2M_\vartheta + 1 \\ 0 & \text{if } r < R \end{cases} \quad (40)$$

This is a trigonometric expansion of order M_ϑ in ϑ and power-type of order d in r ; the total number of multipliers is then $M = 2M_\vartheta + 1 = 2P\sigma + 1$, assuming $\sigma = M_\vartheta/P$.

Figure 10 shows the influence of the σ parameter on \mathcal{E}_{BND} error for two expansion orders $P = 8$ and $P = 22$, and two exponents $d = 1$ and $d = 3$. The asymptotical behaviour is no longer present, with a decreasing error when increasing σ , i.e., increasing the number of multipliers.

This is a positive characteristic of this approach because it allows better convergence rates, as visible in Fig. 11; moreover the convergence rate increases, for both errors $\|\mathcal{E}\|_E$ and \mathcal{E}_{BND} , when increasing the d exponent, in a similar way to the one-dimensional case. However, we

Fig. 10 Immersed boundary error with $M = 2P\sigma + 1$ multipliers

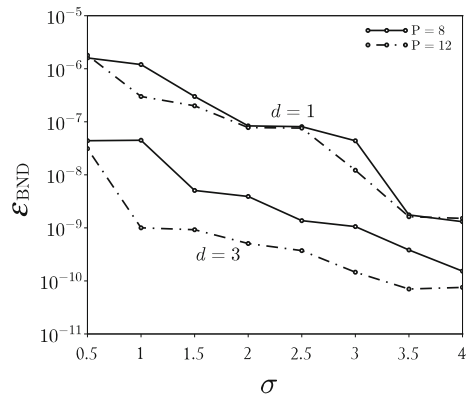
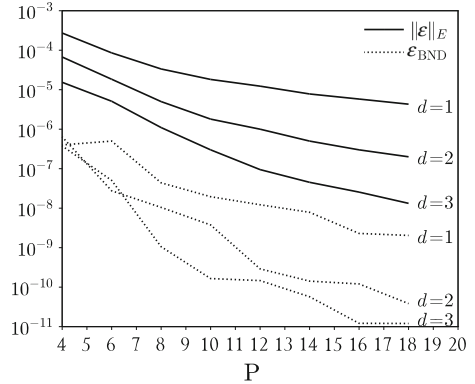


Fig. 11 Case $\sigma = 3$: convergence curves versus polynomial order P



noticed that higher d exponents have a negative influence on the condition number of the multipliers matrix \mathbf{L} .

Graphical representations of the global solution for $P = 18$ and $d = 3$ are given in Fig. 12 where a smoother behaviour of the solution on the fictitious domain can be observed, compared to the previous case.

5.3 Two-Dimensional Biharmonic Equation (Stokes Flow)

5.3.1 Field Equations

The fourth-order biharmonic equation

$$\nabla^4 \psi = 0 \quad (41)$$

arises in many area of physics including continuum mechanics and fluid flow; in fact it can be shown (see [7]) that incompressible two-dimensional Navier–Stokes equations with neglected advective term, i.e., Stokes flow, lead to the following differential system

$$\nabla^2 \psi + \varpi = 0 \quad (42)$$

$$\nabla^2 \varpi = 0 \quad (43)$$

where ψ is the stream function and $\varpi = \nabla \times \mathbf{u}$ is the vorticity of fluid velocity \mathbf{u} ; combining ∇^2 of (42) with (43) yields (41).

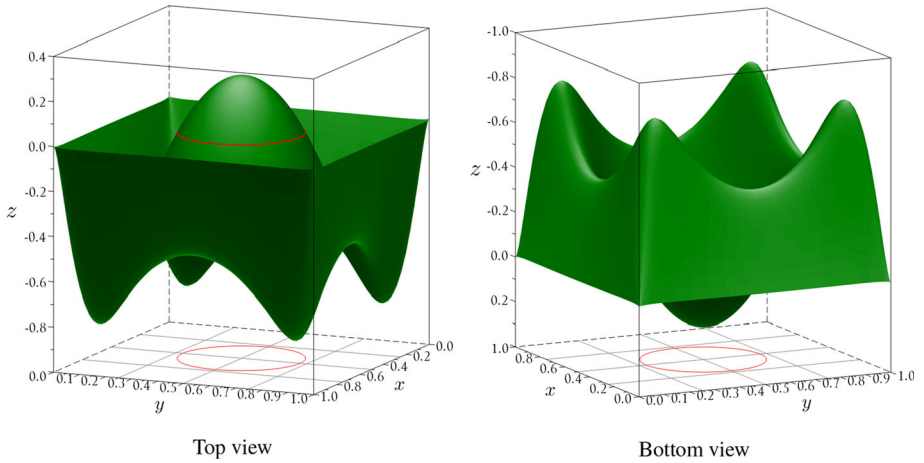


Fig. 12 Global solution with $P = 18$ and $d = 3$

System (42)–(43) is a set of two coupled second-order differential equations that can be solved with the fictitious approach (10)–(14) with $\mathcal{D}_1(\psi, \varpi) = \nabla^2 \psi + \varpi$ and $\mathcal{D}_2(\psi, \varpi) = \nabla^2 \varpi$, source terms $b_1 = b_2 = 0$ and different fictitious source terms $b_{F,1}$ and $b_{F,2}$

$$\mathcal{D}_1(\psi, \varpi) = b_{F,1} \quad (44)$$

$$\mathcal{D}_2(\psi, \varpi) = b_{F,2}. \quad (45)$$

5.3.2 Geometry and Spectral Discretization

The topology of the domains is reported in Fig. 13: the original domain ω is the portion of the unit square outside the circle, the fictitious domain Ω_F is the circle C of radius $R = 0.25$ centered in $(0.5, 0.5)$ and the extended domain $\Omega = \omega \cup \Omega_F$ is therefore the unit square.

The immersed boundary $\gamma_I = \partial C$ is the portion of $\gamma = \partial \omega$ on which constrained BCs will be enforced through distributed multipliers, while regularly enforced BCs will be applied on

Fig. 13 Geometry and domains for the biharmonic equation

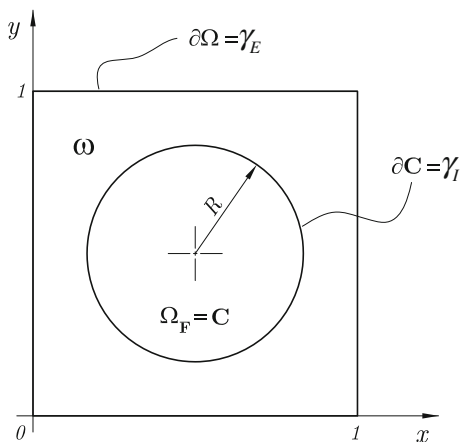
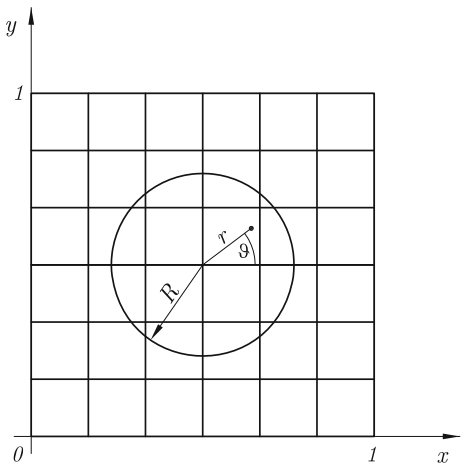


Fig. 14 Domain and discretization for the biharmonic equation



the external boundary $\gamma_E = \partial\Omega$ of the original domain, made by the sides of the unit square (see Fig. 13).

For the spectral/ hp approach we chose 36 elements, 6 for each direction, in order to have at least 4 central elements which are entirely inside the fictitious domain; this arrangement is reported in Fig. 14.

5.3.3 Boundary Conditions

An x -periodic flow is considered, confined by horizontal walls $y = 0$, $y = 1$ and the cylinder C . As a known fact in the stream function-vorticity formulation, double boundary conditions have to be imposed only on ψ at solid walls.

Using the Cartesian coordinate system shown in Fig. 13, the complete set of boundary conditions is

- Periodicity along x : $\psi(0, y) = \psi(1, y)$, $\varpi(0, y) = \varpi(1, y)$ (46)

- Bottom wall $y = 0$: $u = \partial\psi/\partial y = 0$, $v = -\partial\psi/\partial x = 0$ (47)

- Top wall $y = 1$: $u = \partial\psi/\partial y = 0$, $v = -\partial\psi/\partial x = 0$ (48)

- Cylinder wall γ_I : $u_t = \partial\psi/\partial n = 0$, $u_n = -\partial\psi/\partial t = 0$ (49)

where n and t indicate respectively the normal and the tangential directions along γ_I .

From second equation of (47) we have a constant $\psi = c_1$ along the bottom wall; similarly we have $\psi = c_2$ along the top wall and $\psi = c_3$ along cylinder wall γ_I .

The volume flow rate V between the top and bottom walls is given by

$$V = \int_0^1 u(0, y) dy = \int_0^1 \frac{\partial\psi}{\partial y} dy = \psi(0, 1) - \psi(0, 0) = c_2 - c_1 \quad (50)$$

We chose a unit volume flow rate $V = 1$ and a symmetric solution along $y = 0.5$, therefore $c_1 = -0.5$, $c_2 = 0.5$ and $c_3 = 0$.

Boundary conditions given by (46)–(48) have been imposed in the classical way while (49) is the constrained BC along the immersed boundary and has to be enforced through the distributed multipliers technique: (22) and (23) are still valid with $u^* = \psi^*$, $\bar{u} = 0$ and

$\bar{q} = 0$, but the adjustment $\gamma_{I,D} = \gamma_{I,N} = \gamma_I$ is needed to minimize the boundary error along γ_I .

The boundary error $\varepsilon_{\text{BND},\psi}$ between the computed stream function ψ^* and the prescribed value $c_3 = 0$ along γ_I is defined as

$$\varepsilon_{\text{BND},\psi} = \sqrt{\int_{\gamma_I} \psi^{*2} d\gamma} \quad (51)$$

while the boundary error $\varepsilon_{\text{BND},\psi_n}$ between the derivative of the computed stream function $\partial\psi^*/\partial n$ and the prescribed null value along γ_I , first BC of (49), is defined as

$$\varepsilon_{\text{BND},\psi_n} = \sqrt{\int_{\gamma_I} \left(\frac{\partial\psi^*}{\partial n}\right)^2 d\gamma} \quad (52)$$

The total boundary error along γ_I is then $\varepsilon_{\text{BND,tot}} = \varepsilon_{\text{BND},\psi} + \varepsilon_{\text{BND},\psi_n}$.

5.3.4 Analytical Solution

The semi-analytical solution for this problem can be found in [20] where the infinite series solution for stream function ψ has been truncated to the first NP terms and the expansion coefficients have been determined numerically with a least squares approach in order to satisfy the boundary conditions.

Assumed $\varepsilon = \psi^* - \psi$ as the error between computed and semi-analytical stream function, the relative energy norm is again defined as

$$\|\varepsilon\|_E = \sqrt{\int_{\omega} \|\nabla\varepsilon\|_2^2 d\omega}. \quad (53)$$

5.3.5 Fictitious Source Terms b_F

As introduced by (44)–(45), two different source terms $b_{F,1}$ and $b_{F,2}$ are needed

$$b_{F,1} = \sum_{j=1}^{M/2} \lambda_j^{(1)} g_j \quad b_{F,2} = \sum_{j=1}^{M/2} \lambda_j^{(2)} g_j \quad (54)$$

where M is even and the functions g_j are the same for both expansions and satisfy $g_j = 0$ on ω ; therefore the total number of unknown multipliers $\lambda_j^{(1)}$ and $\lambda_j^{(2)}$ is still M .

Fictitious functions g_i defined on internal elements The g_i functions defining the fictitious source terms $b_{F,1}$ and $b_{F,2}$ in (54) are non-zero only on the four central elements A, B, C and D of Fig. 15, which are the elements entirely inside the fictitious domain Ω_F , and therefore these elements don't intersect the immersed boundary.

More precisely, on each of these 4 elements we define $2M_e$ functions g_j : M_e assuming a unit constant value on each parallel horizontal strip and M_e assuming a unit constant value on each parallel vertical strip, covering the whole element as reported in Fig. 15; therefore we have $M/2 = 8M_e$ and we define $\sigma = M/(16P) = M_e/P$.

Figure 16 shows the influence of the σ parameter on both the ε_{BND} boundary errors (for ψ and ψ_n) along the immersed boundary for two expansion orders $P = 8$ and $P = 16$. σ values greater than 1 have a little influence on the boundary error, which possesses an

Fig. 15 Graphical representation of g_j functions for fictitious source terms

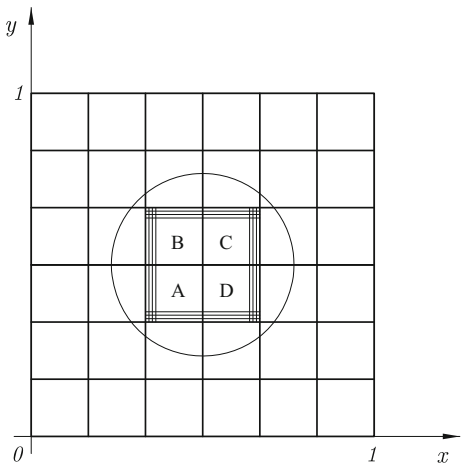
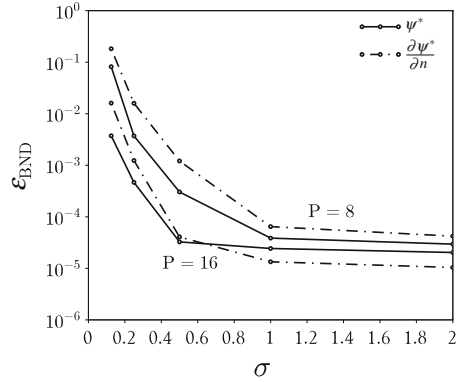


Fig. 16 Immersed boundary error with $M = 2P\sigma$ multipliers



asymptotical behaviour. As in the analogous Poisson 2D problem, for a fixed value of P (polynomial expansion order) it's impossible to satisfy the constrained BC on the immersed boundary with arbitrary accuracy even using a very high number M of multipliers.

Graphical representations of the stream function for $P = 16$ are given in Fig. 17 where the particular maximum and minimum peaks of the solution on the fictitious domain can be observed.

Fictitious functions g_i defined on Ω_F Similarly to the Poisson 2D problem, we now propose another possible choice for g_i fictitious functions which allows a better resolution of the BCs along the immersed boundary; using the polar coordinates (r, ϑ) shown in Fig. 14, g_i functions are defined as

$$g_i(r, \vartheta) = \begin{cases} r(r-R)^d \sin(i\vartheta) & i = 1, \dots, M_\vartheta \\ r(r-R)^d \cos[(i - M_\vartheta - 1)\vartheta] & i = M_\vartheta + 1, \dots, 2M_\vartheta + 1 \\ 0 & \text{if } r > R \end{cases} \quad (55)$$

This is again a trigonometric expansion of order M_ϑ in ϑ and power-type of order $d + 1$ in r ; the initial r factor is necessary to get rid of the singularity of trigonometric functions in $r = 0$.

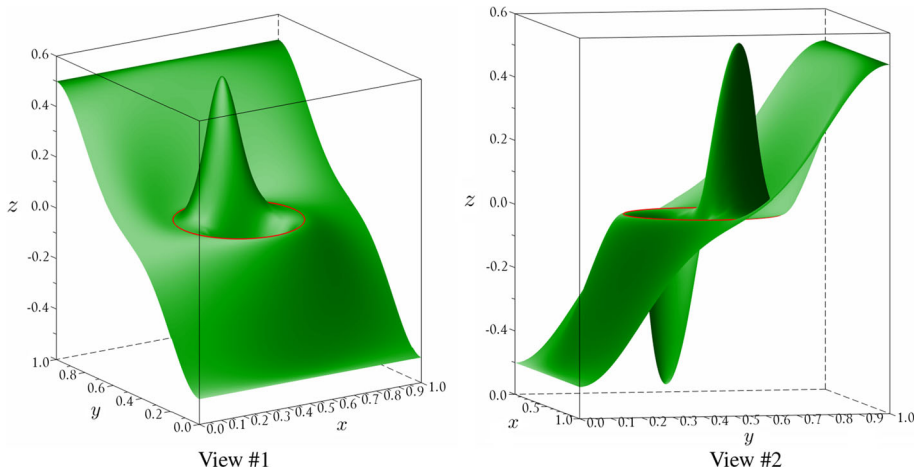
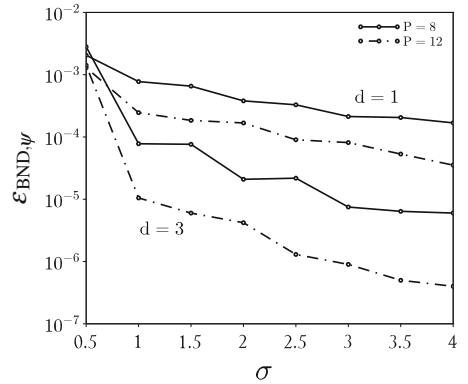


Fig. 17 Global stream function ψ with $P = 16$

Fig. 18 Immersed boundary error for stream function ψ with $M = 2(2M_\vartheta + 1)$ multipliers



We have $2M_\vartheta + 1$ fictitious functions and therefore the total number of multipliers is $M = 2(2M_\vartheta + 1)$; again, we define $\sigma = M_\vartheta / P$.

Figures 18 and 19 shows the influence of the σ parameter on both $\varepsilon_{\text{BND},\psi}$ and $\varepsilon_{\text{BND},\psi/n}$ boundary errors along γ_I for two expansion orders $P = 8$ and $P = 12$ and two exponents $d = 1$ and $d = 3$.

The behaviour of these errors is similar to those of the analogous bi-dimensional Poisson problem: there is an almost-continuously decreasing behaviour for both errors when increasing σ and d parameters.

Figure 20 shows the convergence curves of the $\varepsilon_{\text{BND,tot}}$ immersed boundary total error and $\|\varepsilon\|_E$ global error for $\sigma = 3$: it is possible to see the positive influence of the d exponent on the convergence rates.

However, analogously to the bi-dimensional Poisson problem, we report a negative influence of the d exponent on the condition number of the multipliers matrix \mathbf{L} , which heavily affects the accuracy of the computed solution with this formulation.

A graphical representation of the stream function for $P = 18$ and $d = 3$ is given in Fig. 21 where, again, the particular maximum and minimum peaks of the solution on the fictitious domain can be observed.

Fig. 19 Immersed boundary error for stream function derivative ψ_n with $M = 2(2M_\vartheta + 1)$ multipliers

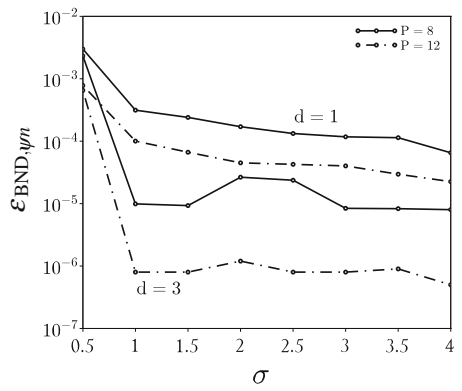


Fig. 20 Case $\sigma = 3$: convergence curves versus polynomial order P

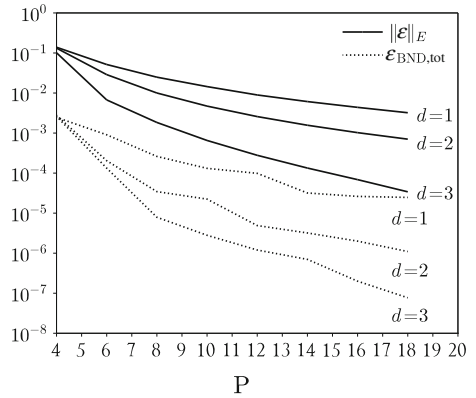
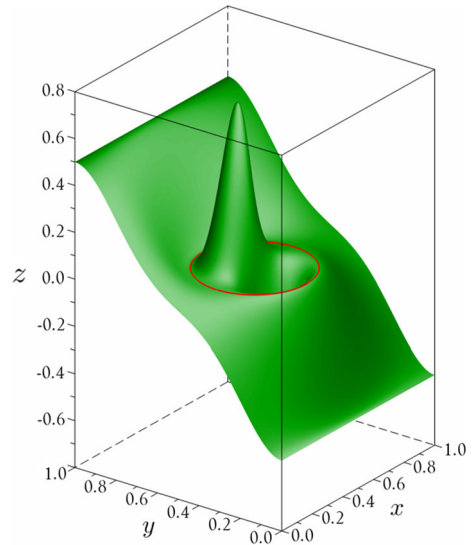


Fig. 21 Global stream function ψ with $P = 18$ and $d = 3$



6 Conclusions

An approach for solving linear second-order differential problems over irregularly-shaped domains is proposed; this approach, based on fictitious domain method and spectral/ hp element discretization, employs distributed Lagrange multipliers (fictitious functions) to enforce boundary conditions on the immersed boundary. We presented the formulation of this approach and its application to specific test cases; we considered a one-dimensional Poisson problem, a two-dimensional Poisson problem and a Stokes flow problem (biharmonic equation). For each case specific distributed Lagrange multipliers were introduced, analyzing the convergence properties of each choice.

In each test good results have been obtained in terms of convergence rate of the computed solution to the exact (analytical) one; in several cases it has been possible to obtain a convergence rate comparable to the ideal spectral rate that is lost when impulsive Lagrange multipliers are employed within classical high order fictitious domain approaches [9].

Alongside this favorable feature there is the disadvantage of an appropriate definition of the distributed Lagrange multiplier functions, defined over the fictitious domain. However, further analysis have to be carried out in order to ensure that the proposed approach can be an innovative and effective tool for the accurate solution of complex problems defined over general shaped domains with irregularities (corners, holes, etc.); its application could bring great advantages to the solution of problems with moving bodies and both shape and topology optimization problems.

References

1. Peskin, C.S.: Flow patterns around heart valves: a digital computer method for solving the equations of motion. PhD thesis, Sue Golding Graduate Division of Medical Sciences, Albert Einstein College of Medicine, Yeshiva University (1972)
2. Glowinski, R., Pan, T.W., Periaux, J.: A fictitious domain method for external incompressible viscous flow modeled by Navier–Stokes equations. *Comput. Methods Appl. Mech. Eng.* **112**(1–4), 133–148 (1994a)
3. Glowinski, R., Pan, T.W., Periaux, J.: A fictitious domain method for Dirichlet problem and applications. *Comput. Methods Appl. Mech. Eng.* **111**(3–4), 283–303 (1994b)
4. Glowinski, R., Pan, T.W., Periaux, J.: A Lagrange multiplier/fictitious domain method for the Dirichlet problem—generalization to some flow problems. *Japan J. Indust. Appl. Math.* **12**, 87–108 (1995)
5. Babuška, I., Guo, B.: The $h - p$ version of the finite element method. *Comput. Mech.* **1**(1), 21–41 (1986)
6. Babuška, I., Suri, M.: The $h - p$ version of the finite element method with quasiuniform meshes. *ESAIM Math. Model. Numer. Anal.* **21**(2), 199–238 (1987)
7. Karniadakis, G., Sherwin, S.: *Spectral/ hp Element Methods for Computational Fluid Dynamics*. Oxford University Press, New York (1999)
8. Pontaza, J., Reddy, J.: Space-time coupled spectral/ hp least-squares finite element formulation for the incompressible Navier-Stokes equations. *J. Comput. Phys.* **197**(2), 418–459 (2004)
9. Vos, P., Van Loon, R., Sherwin, S.J.: A comparison of fictitious domain methods appropriate for spectral/ hp element discretization. *Comput. Methods Appl. Mech. Eng.* **197**(25), 2275–2289 (2008)
10. Parussini, L.: Fictitious domain approach for spectral/ hp element method. *Comput. Model. Eng. Sci.* **17**(2), 95–114 (2007)
11. Parussini, L.: Fictitious domain approach via Lagrange multipliers with least squares spectral element method. *J. Sci. Comp.* **37**(3), 316–335 (2008)
12. Parussini, L., Pediroda, V.: Fictitious domain with least-squares spectral element method to explore geometric uncertainties by non-intrusive polynomial chaos method. *Comput. Model. Eng. Sci.* **22**(1), 41–64 (2007)
13. Parussini, L., Pediroda, V.: Investigation of multi geometric uncertainties by different polynomial chaos methodologies using a fictitious domain solver. *Comput. Model. Eng. Sci.* **23**(1), 29–52 (2008)
14. Glowinski, R., Pan, T.W., Periaux, J.: Distributed Lagrange multiplier method for incompressible viscous flow around moving rigid bodies. *Comput. Methods Appl. Mech. Eng.* **151**(1–2), 181–194 (1998)

15. Auricchio, F., Boffi, D., Gastaldi, L., Lefieux, A.: On a fictitious domain method with distributed Lagrange multiplier for interface problems. *Appl. Numer. Math.* **95**, 36–50 (2015)
16. Boffi, D., Cavallini, N., Gastaldi, L.: The finite element immersed boundary method with distributed Lagrange multiplier. *SIAM J. Numer. Anal.* **53**(6), 2584–2604 (2015)
17. Glowinski, R.: Finite element methods for incompressible viscous flow. In: *Handbook of Numerical Analysis*, chap 8, vol. 9, pp. 3–1176. North-Holland, Amsterdam (2003)
18. Dong, S., Liu, D., Maxey, M.R., Karniadakis, G.E.: Spectral distributed Lagrange multiplier method: algorithm and benchmark tests. *J. Comput. Phys.* **195**(2), 695–717 (2004)
19. Buffat, M., Le Penven, L.: A spectral fictitious domain method with internal forcing for solving elliptic pdes. *J. Comput. Phys.* **230**(7), 2433–2450 (2010)
20. Moreau, F., Hellou, M., El Yazidi, M.Z.: Ecoulements cellulaires de Stokes dans un canal plan obstrué par une file de cylindres. *Angew. Math. Phys.* **49**(1), 31–45 (1998)